ResearchGate

See discussions, stats, and author profiles for this publication at: https://www.researchgate.net/publication/51628091

Efficient Blue-Emitting Ir(III) Complexes with Phosphine Carbanion-Based Ancillary Ligand: A DFT Study

ARTICLE *in* THE JOURNAL OF PHYSICAL CHEMISTRY A · SEPTEMBER 2011

Impact Factor: 2.69 · DOI: 10.1021/jp200878y · Source: PubMed

CITATIONS
20

READS
45

4 AUTHORS, INCLUDING:

Jian Wang
Jilin University
66 PUBLICATIONS **188** CITATIONS
SEE PROFILE

Fu-Quan Bai
Jilin University
124 PUBLICATIONS **435** CITATIONS
SEE PROFILE

Available from: Jian Wang
Retrieved on: 24 January 2016

THE JOURNAL OF PHYSICAL CHEMISTRY A

ARTICLE

pubs.acs.org/JPCA

Efficient Blue-Emitting Ir(III) Complexes with Phosphine Carbanion-Based Ancillary Ligand: A DFT Study

Jian Wang,[†] Fu-Quan Bai,[†] Bao-Hui Xia,[†,‡] and Hong-Xing Zhang*[,†]

[†]State Key Laboratory of Theoretical and Computational Chemistry, Institute of Theoretical Chemistry, Jilin University, Changchun 130023, People's Republic of China

[‡]College of Chemistry, Jilin University, Changchun 130000, People's Republic of China

ABSTRACT: We report a theoretical study on a series of heteroleptic cyclometalated Ir(III) complexes for OLED application. The geometries, electronic structures, and the lowest-lying singlet absorptions and triplet emissions of [$(fppy)_2$Ir(III)-(PPh_2Np)] (**1**), and theoretically designed models [$(fppy)_2$-Ir(III)(PH_2Np)] (**2**) and [$(fppy)_2$Ir(III)$Np]^-$(**3**) were investigated with density functional theory (DFT)-based approaches, where, fppyH = 4-fluorophenyl-pyridine and NpH = naphthalene. The ground and excited states were, respectively, optimized at the M062X/LanL2DZ;6-31G* and CIS/LanL2DZ:6-31G* level of theory within CH_2Cl_2 solution provided by PCM. The lowest absorptions and emissions were evaluated at M062X/Stuttgart;cc-pVTZ;cc-pVDZ level of theory. Though the lowest absorptions and emissions were all attributed as the ligand-based charge−transfer transition with slight metal-to-ligand charge−transfer transition character, the subtle differences in geometries and electronic structures result in the different quantum yields and versatile emission color. The newly designed molecular **3** is expected to be highly emissive in deep blue region.

INTRODUCTION

Phosphorescent materials based on heavy transition metal complexes, particularly the iridium complex, have attracted much attention due to their potential application as highly efficient electron luminescent emitters in organic light emitting diodes (OLED).[1−7] Several research groups have adopted heteroleptic cyclometalated Ir(III) complex in OLED and obtained up to 19% external quantum efficiency.[8] These successful applications mainly benefit from[9] (i) the larger d-orbital splitting compared with the other metals in the series; (ii) the closely lying $\pi-\pi^*$ orbitals and MLCT state; (iii) the stronger heavy atom effect (namely, the larger spin−orbit coupling effect constant of Ir atom,[10] ξ = 3909 cm^{-1}) that enhances the spin−orbit coupling, giving a much allowed T_1-S_0 transition and, hence, a higher quantum yield.

Because the report that the efficiency of $Ir(ppy)_3$ (ppyH = 2-phenyl-pyridine) based OLED can exceed 80%,[11] enormous efforts have been devoted in developing other Ir(III) cyclometalated complexes with even higher efficiency for OLED application.[12−18] Theoretically, the 100% internal quantum efficiency can be achieved because the existence of iridium atom that allows efficient harvesting of electroluminescence originating from both singlet and triplet excitations. In the past 10 years heteroleptic Ir(III) complexes comprising stable ancillary chelates such as acetylacetonate (acac),[19,20] picolinate (pic),[21] functionalized azolate,[22] dithiocarbamate,[23] and benzamidinate[24] have been investigated to find out the perfect one with the 100% internal quantum efficiency but in vain. Recently, the heteroleptic cyclometalated Ir(III) complex for which the ancillary ligand is derived from the carbanion based ligand has been reported[25] and the internal quantum efficiency up to 100% can be achieved for the heteroleptic Ir(III) phosphor complexes with the P̂C ancillary ligand,[26] where, P̂C = benzyldiphenylphosphine. Despite of the above-mentioned extensive examination, the relationship between structural and spectroscopic properties remains a major challenge.[27]

On the other hand, true blue light emission could make OLED displays the next big thing in consumer electronics. But if it were that simple. One of the reasons why current OLED displays are not as popular as liquid crystal display (LCD) and light−emitting diode (LED) displays is that the blue emitters have poor color quality and low external quantum efficiency. Blue light has a wider band gap that requires higher energy for effective blue light emission, and inherently has lower efficiency and a shorter lifetime. Improvements to the efficiency and lifetime of blue OLEDs is vital to the success of OLEDs as replacements for LCD technology. Considerable research has been invested in developing blue OLEDs with high external quantum efficiency as well as a deeper blue color.[28,29] External quantum efficiency values of 20 and 19% have been reported for red (625 nm) and green (530 nm) diodes, repectively.[30,31] However, blue diodes (430 nm) have only been able to achieve maximum external quantum

Received: January 27, 2011
Revised: September 2, 2011
Published: September 08, 2011

ACS Publications © 2011 American Chemical Society

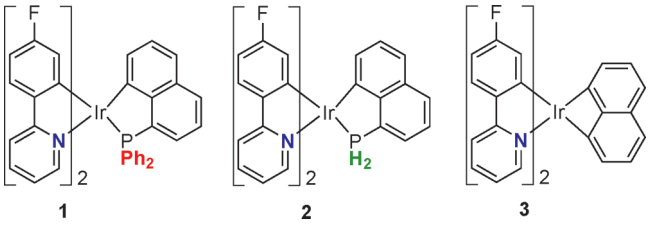

Figure 1. Schematic representation of **1**−**3**.

efficiencies in the range between 4 and 6%.[32] High efficiency, long lifetime, and pure blue emitter is the most wanted for practical OLED application.

On the theoretical side, the reliability and accuracy of computation chemistry are widely recognized nowadays.[33−39] One would like to predict beforehand the potential properties of possible emitters to screen out configurations without the desired qualities and find those systems worthy of experimental testing. Indeed, computational studies can help us realize the assumption and provide some hints about some vital aspects of the system under investigation.

With the above backgrounds in mind, theoretical calculations were carried out to search for possible highly emissive blue emitter based on the detailed analysis of electronic structure of the newly reported Ir(III) cyclometalated complex $[(fppy)_2Ir(III)(PPh_2Np)]$ (denoted as **1**) with density functional theory (DFT)[40,41] based methods, where fppyH = 4-fluorophenylpyridine and NpH = naphthalene (see Figure 1). By comparing the electronic properties and excitation energy of **1** with theoretical designed molecular $[(fppy)_2Ir(III)(PH_2Np)]$ (denoted as **2**) and $[(fppy)_2Ir(III)(Np)]$ (denoted as **3**, see Figure 1), we were happy to announce that **3** would be a highly efficient blue emitter.

COMPUTATIONAL DETAILS

All calculations have been performed with Gaussian09 suite of program[42] with a tight self-consistent field convergence threshold for both gradient and wave function convergence. We have followed a well-established three-step approach: (i) to optimize the ground and excited state geometries until the residual mean force is smaller than 1.0×10^{-5} au (the so-called tight threshold in Gaussian); (ii) the vibrational frequency calculation to confirm the optimized structures are a true minimum; and (iii) moving on from the optimized ground and excited state geometries, to calculate the respective singlet−singlet and singlet−triplet excitation energies with time-dependent DFT (TD-DFT) approach.[43]

Because the experimental geometry and spectral data are obtained in solid phase and in CH_2Cl_2 solution, respectively, we have considered solvent effects in geometry optimization and Hessian calculations by means of the well-known Polarizable Continuum Model (PCM)[44,45] with the default parameters embedded in Gaussian09 to obtain a valid approximation of chemical environment.

In terms of basis sets, the double-ζ quality 6-31G* and LanL2DZ were employed for the lighter nonmetallic atoms in ligands (such as C, N, F, P, and H atoms) and the Ir atom, respectively. A relativistic effective core potential (ECP) for Ir atom replaces the inner core electrons[46] leaving the outer layer $[(5s^2)(5p^6)]$ electrons and the $(5d^6)$ valence electrons. This combination of basis set is adequate to describe the ground and excited state geometries of the Ir(III) complexes, and it has been verified and discussed elsewhere.[47,48] To describe the excitation energy and excited state electronic transition properties accurately and reasonably, all TD-DFT calculations were assessed with a fairly large basis set: Stuttgart relativistic small-core effective potential[49−51] for Ir; triplet-ζ plus polarization basis set (cc-pVTZ)[52] for the C, N, F, and P atoms; and double-ζ plus polarization basis set (cc-pVDZ)[52] for H atoms.

Table 1. Optimized Geometry Parameters of 1 in Ground State: Percent Error (δ) versus xc Functionals

		B3LYP		M062X	
item	expt[a]	cal.	δ	cal.	δ
		Bond Length, Å			
Ir−C1[b]	2.1086	2.1419	1.6	2.1129	0.2
Ir−C2	2.0186	2.0364	0.9	2.0065	0.6
Ir−C3	2.0812	2.1073	1.3	2.0851	0.2
Ir−N1	2.1033	2.1253	1.0	2.1264	1.1
Ir−N2	2.1422	2.1973	2.6	2.2009	2.7
Ir−P	2.2424	2.3111	3.1	2.2491	0.3
		Bond Angle, °			
P−Ir−C1	82.3	81.0	1.5	81.1	1.4
N1−Ir−C2	79.7	79.4	0.4	80.0	0.4
N2−Ir−C3	78.2	77.5	0.9	77.7	0.6
C1−Ir−N2	97.6	97.6	0.0	98.5	0.9
C1−Ir−C2	85.6	86.4	0.9	86.1	0.6
C2−Ir−C3	98.6	98.5	0.1	97.5	1.1
N1−Ir−P	174.4	173.7	0.4	172.7	1.0

[a] See ref 26. [b] For labeling scheme, see Figure 2.

The newly developed M062X exchange-correlation functional has been applied to optimize the ground state geometries of the three complexes in CH_2Cl_2 solution with no symmetry constraint. The geometries of the lowest triplet excited state were evaluated by the configuration interaction singles (CIS)[53,54] method, the triplet excited state being related to the emission process. The M062X functional[55] together with the larger basis set mentioned above were adopted to evaluate the lowest singlet−singlet and singlet−triplet excitation energies and electronic transition nature. It should to be noticed that the oscillator strengths of singlet−triplet excitations are set to zero due to the neglect of spin−orbital coupling in the triplet TD-DFT calculations in Gaussian09.

RESULTS AND DISCUSSION

Methodology. A crucial step in theoretical investigations employing DFT is the choice of an appropriate exchange-correlation (xc) functional and a reasonable basis set.[56] Given the recent studies and the growing applications of DFT methods in electronic states,[57−61] it is important to investigate their applicability for studying transition metal complexes and, if necessary, identify low-cost alternative methods. To this end, in present work we examined the accuracy of two xc functionals, which provided favorable application in heavy atom molecules and weak interaction. Thus, with experimentally detected geometry data in hand, complex **1** was taken as the reference molecule to screen out the suitable functional for current investigation. To this end, the well-established hybrid xc functionals Becke3−Lee−Yang−Parr (B3LYP)[62] and the newly developed M062X were selected to do the benchmark test.

The optimized ground state geometry data together with the X-ray crystal diffraction data[26] of **1** are reported in Table 1. On the one hand, the percent error (δ) indicates that the M062X functional provides a slight higher accuracy (little δ) than B3LYP functional in prediction of bond length despite of similar error levels in prediction of bond angles. On the other hand, the bond lengths optimized with M062X functional are consistent with the corresponding experimental values except a deviation below 0.059 Å for the calculated bond distance Ir−N2 (2.2009 Å) from the X-ray result. The discrepancy of bond length and angle between the calculated and measured values is reasonable and acceptable since the chemical environments of the complex are different in the two cases: in experiment, the molecule is in a tight crystal lattice, whereas in present calculation the molecule is confined in a solvent field that is simulated by PCM. In conclusion, the current level of theory (M062X/LanL2DZ;6-31G*) is sufficient and reliable in geometry calculation. Therefore, both the singlet and the triplet excitation energies were all evaluated within M062X functional but with larger basis set to describe the electron−exchange correlation for current system as accurately as possible.

Geometries in Ground and Excited States. The main optimized geometry parameters of **1**−**3** in singlet ground state (S_0) and lowest-lying triplet excited state (T_1) are summarized in Table 2, and the optimized stable structures of **1**−**3** are shown in Figure 2. The calculated vibrational frequencies with no imaginary frequency based on the optimized geometries for **1**−**3** verify that each of the optimized structure is a true minimum on the potential energy surface.

The three complexes maintain the quasi-octahedral geometry as being observed in other typical six-coordinated Ir(III) complexes.

Table 2. Main Optimized Geometry Parameters of 1−4 in Singlet Ground State (S_0) and Lowest-Lying Triplet Excited State (T_1) at M062X/LanL2DZ;6-31G* and CIS/LanL2DZ;6-31G* Level of Theory, Respectively

	1		2		3	
item	S_0	T_1	S_0	T_1	S_0	T_1
Ir−N1	2.126	2.143	2.114	2.135	2.182	2.202
Ir−N2	2.201	2.206	2.203	2.210	2.205	2.215
Ir−C1	2.112	2.141	2.115	2.151	2.177	2.192
Ir−C2	2.007	2.060	1.999	2.047	1.973	2.030
Ir−C3	2.085	2.119	2.080	2.111	2.037	2.093
Ir−C4					2.028	2.086
Ir−P	2.249	2.369	2.226	2.313		

Yet, it should be noted that there are subtle differences among the structural parameters of **1**−**3**. First, as far as **1** and **2** are concerned, the difference in space arrangement between Ir atom and the ligands is caused by the size of ligand, in other words, the steric hindrance of ancillary ligands. The absence of the phenyl group in the naphthyl-phosphine (P̂C) ligand reduces the steric hindrance between the diphenyl(1-naphthyl)phosphine (PPh_2Np) ligand and the fppy ligand greatly; making it is easier for electrons in the naphthyl-phosphine (PH_2Np) ligand and Ir atom to communicate with each other. Therefore the coordination interaction between Ir and P atoms would be stronger in **2**, compared with that in **1**. Namely, it is reasonable that the Ir−P bond length is shorter in **2** than it was in **1**. Second, smaller P̂C ligand results in a closer arrangement of Ir metal center and ligands in **2**. Compared with **1**, the shorter distance between Ir metal center and ligands may facilitate the charge−transfer transition between the metal center and ligands, eventually benefit the quantum yield.

Moreover, in **1** the naphthyl group (Np) of the phosphine ligand shows parallel arrangement to fppy chelate, for which the centroid−centroid distance between the inner hexagonal ring of Np and pyridine fragment is calculated to be 3.134 Å. Such non-negligible intraligand $\pi-\pi$ stacking interaction is also observed in experiment[26] and other similar cyclometalated Ir(III) complexes bearing 2-(diphenylphosphino)phenolate chelate.[63]

The goemetry in triplet excited state basically keeps the same as it was in singlet ground state. In triplet excited state, however,

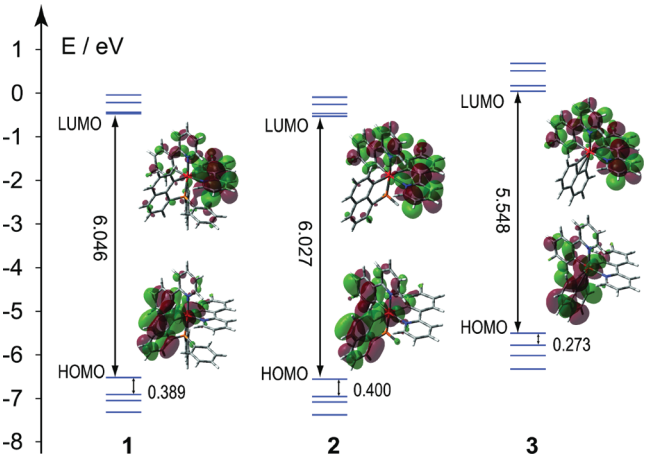

Figure 3. Calculated electronic structure in CH_2Cl_2 for **1**−**3** at M062X/Stuttgart;cc-pVTZ;cc-pVDZ level of theory. Also shown are isodensity surface plots of HOMO and LUMO for **1** − **3**.

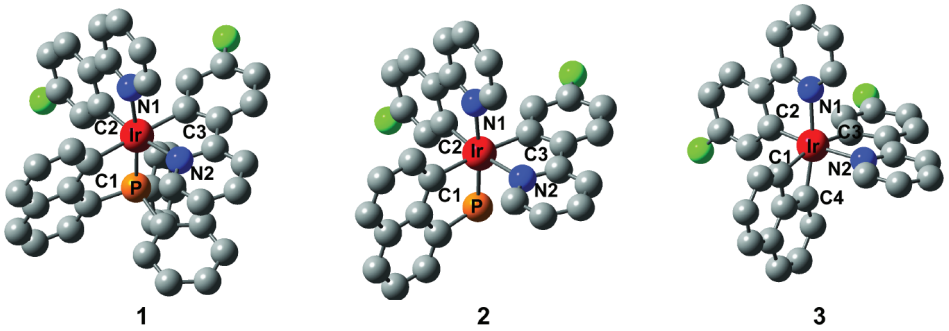

Figure 2. Optimized ground state structure of **1**−**3** at M062X/LanL2DZ;6-31G* level of theory. Hydrogen atoms were omitted for clarity.

dx.doi.org/10.1021/jp200878y |J. Phys. Chem. A 2011, 115, 11689–11695

Table 3. Molecular Orbital Composition (%) of 1 in Ground State, M062X/Stuttgart;cc-pVTZ;cc-pVDZ Level of Theory

orbital	Ir	fppy-1	fppy-2	Np	PPh_2
L+3	13	22	29	14	22
L+2	7	17	8	45	23
L+1	14	49	16	18	3
LUMO	6	15	54	7	17
HOMO	34	14	9	40	3
H-1	16	26	26	27	5
H-2	21	11	45	17	7
H-3	9	31	31	25	4

Table 4. Molecular Orbital Composition (%) of 2 in Ground State, M062X/Stuttgart;cc-pVTZ;cc-pVDZ Level of Theory

orbital	Ir	fppy-1	fppy-2	Np	PH_2
L+3	13	28	29	29	1
L+2	5	5	14	64	11
L+1	9	50	27	14	0
LUMO	10	30	52	6	2
HOMO	36	17	9	37	1
H-1	12	19	26	43	1
H-2	26	17	46	9	2
H-3	7	31	37	25	1

these three molecules show a slight expansion in size, namely, the distances between the Ir metal center and ligands are enlarged slightly, see Table 2. These subtle differences in structure can be ascribed to the different electronic structures between the singlet ground state and the triplet excited state. These structures constitute the starting point of the results reported herein.

Frontier Molecular Orbital Properties. To provide insight into the electronic structures of **1**−**3**, we report in Figure 3 the results of natural bond orbital (NBO) population calculation performed at the optimized S_0 geometries in CH_2Cl_2 solution together with the plots of the highest occupied molecular orbital (HOMO, H) and the lowest occupied molecular orbital (LUMO, L) for these Ir(III) complexes. The molecular orbital compositions of **1**−**3** are reported in Tables 3−5, respectively.

The electronic structures of **1** and **2** are rather similar due to the similarity in geometry, yet there are sizable differences in orbital composition of both occupied and unoccupied orbitals. The HOMOs of **1** and **2** are almost isolated orbital (see Figure 3) composed by a combination of d orbital of Ir and π orbitals of the naphthyl moiety of the $\hat{P}C$ ligand (Np), see Tables 3 and 4, and are calculated at −6.521 and −6.557 eV for **1** and **2**, respectively. The contribution of Ir orbital to the HOMOs varies from 34% in **1** to 36% in **2**. The HOMOs of **1** and **2** are followed, in order of decreasing energy, by two closely lying, almost degenerated combination of π orbitals of fppy and Np ligands and d orbitals of Ir atom, but the closely lying π orbitals are missing in **3**. The HOMO-1 is calculated to lie 0.389 and 0.400 eV bellow the HOMOs of **1** and **2**, respectively. The LUMOs of **1** and **2** are π^* orbitals localized on the fppy ligands and calculated to lie at −0.475 and −0.530 eV, respectively. The almost degenerated couple LUMO and L+1 can stabilize the excited electrons easily, which makes **1** and **2** have a better capability in holding the excited electrons, finally benefits electron transportation process.

Table 5. Molecular Orbital Composition (%) of 3 in Ground State, M062X/Stuttgart;cc-pVTZ;cc-pVDZ Level of Theory

orbital	Ir	fppy-1	fppy-2	Np
L+3	4	59	37	0
L+2	3	37	59	1
L+1	3	66	31	1
LUMO	2	31	67	0
HOMO	20	9	3	69
H-1	25	25	11	39
H-2	47	7	40	5
H-3	26	3	18	53

The HOMO of **3** is a combination of d orbital of Ir and π orbital of Np ligand with the contribution of 20 and 69%, respectively. Compared with those of **1** and **2**, the HOMO of **3** is destabilized due to the direct coordination between Ir and Np ligand, and the latter acts as a strong electron donor. The strong destabilization of the HOMO in **3** not only reflects on the energies of the occupied orbitals but also the energies of the unoccupied orbitals. As a result, the gaps between the HOMO and the H-1/H-2 couple decrease effectively in **3** compared with that in **1** and **2**. The almost degenerated couple LUMO and L+1 are absent in **3**.

In short, the electron populations in **1**−**3** are identical. For **1** and **2**, they are analogous to each other not only in charge population but also in molecular orbital energy levels. Whereas both the occupied and virtual orbitals of **3** are destabilized with respect to that of **1** and the energy gaps between the two adjacent occupied or virtual orbitals are relatively large. It is worth mentioning that it is not straightforward to compare the calculated HOMO−LUMO gap of **1** with the corresponding quantities measured by electrochemical studies (6.046 vs 2.86). Because the calculated values are approximations to vertical oxidation/reduction potentials, while the electrochemical potentials refer to adiabatic processes, in which both the oxidized and the reduced species are at their respective equilibrium configurations. Additionally, our data reveals that the reduction process of **1** would occur on the fppy ligand, which agrees with what has been observed in experiment.

Lowest-Lying Singlet Absorption and Triplet Emission. The calculated lowest singlet absorptions and triplet emissions of **1**−**3** associated with their oscillator strengths, the main electronic transitions, and the corresponding assignments are summarized in Table 6. The calculated lowest-lying absorption at 320 nm and emission at 566 nm are comparable to the experimental value,[26] 354 and 574 nm, respectively.

For **1**, the lowest-lying singlet−singlet transitions are primarily attributed to HOMO → L+1 excitation, in which the HOMO of **1** is mainly localized at the Np of ancillary phosphine chelate and the central metal atom, while the electron density of L+1 is distributed among the fppy, Np ligands and Ir metal center. Therefore, the $S_0 \rightarrow S_1$ transition of **1** involves concomitantly ligand-based charge−transfer transition (LLCT) and metal-to-ligand charge−transfer transition (MLCT) characteristics. Because of the similar geometry and electronic structure of **1** and **2**, and the identical electronic configurations of LUMO and L+1 in **2**,

Table 6. Calculated Lowest-lying Singlet Absorptions and Triplet Emissions (λ_{cal}, nm), Oscillator Strength (f), Orbital Transition Analysis, and Metal Character (M%) of 1−3, M062X/Stuttgart;cc-pVTZ;cc-pVDZ Level of Theory

	states	λ_{cal}	f	transition	contrib. (%)	nature	M %
1	S_1	320	0.1476	H → L+1	73	ILCT/MLCT	15
	T_1	566	0	H → L	93	^{3}ILCT/^{3}LMCT	16
2	S_1	322	0.1515	H → L+1	52	ILCT/MLCT	14
				H → L	28	LLCT/MLCT	7
	T_1	563	0	H → L	94	^{3}ILCT/^{3}LMCT	19
3	S_1	351	0.1353	H → L+1	22	LLCT/MLCT	4
				H → L	31	LLCT/MLCT	6
				H-1 → L+1	15	ILCT/MLCT	3
				H-1 → L	22	LLCT/MLCT	5
	T_1	470	0	H → L+1	24	^{3}MLCT/^{3}LLCT	13
				H → L	75	^{3}MLCT/^{3}LLCT	37

the $S_0 \rightarrow S_1$ transition character for **2** is identical to that of **1**. And the lowest-lying absorptions of the two complexes are almost in duplicate: 322 nm in **2** vs 320 nm in **1**.

Due to the decreased HOMO−LUMO gap, see Figure 3, the original $S_0 \rightarrow S_1$ absorption of **1** at 320 nm is red-shifted to 351 nm in **3**. There are several transitions which contribute to the 354 nm singlet absorption in **3**, see Table 6. According to the frontier orbital analysis, the virtual orbitals of **3** are almost localized on fppy ligands while the HOMO is delocalized on Ir metal (20%) and Np ligand (69%). And the H-1 of **3** is almost populated equally on Ir metal and both fppy and Np ligands, see Table 5. Therefore it is sensible to assign the 354 nm absorption as ligand-based charge−transfer transition and metal-to-ligand charge−transfer transition characteristics.

From **1** to **3**, the emission peaks are blue-shifted from 566 nm in **1** to 563 and 470 nm in **2** and **3**, respectively, In **1** the transition HOMO → LUMO controls the experimentally observed emission. According to our calculation, the P̂C ligand masters the LUMO of **1** with 79% contribution, while the HOMO is delocalized on Ir metal (23%) and P̂C ligand (66%). Therefore, the observed emission can be assigned as interligand charge−transfer (ILCT) transition within P̂C ligand but mixed with little contribution of ligand-to-metal charge−transfer (LMCT) transition from π^* orbital of P̂C ligand to d orbital of Ir metal. Because the electronic structure of **1** and **2** are similar in nature, the luminescent property of **2** is homologous to **1**.

As far as **3** is concerned, it is a bit different in emission character. There are two transitions contributing to the calculated emission at 470 nm. In triplet excited state the LUMO and L+1 are mastered by the d orbital of Ir metal, while the HOMO is delocalized on Np ligand (63%) and d orbital of Ir (21%). Therefore, this emission can be assigned as ^{3}MLCT mixed with ^{3}LLCT.

Theoretical Expectation of Quantum Yield. The geometrical difference leads to interesting influence on quantum yields and hence the relaxation dynamics. In the above section, we have proved the newly designed theoretical model **2** is identical in electronic structure properties and charge−transfer transition characteristics with the experimentally synthesized molecular **1**. And what's more, it has been reported that **1** is highly emissive.[26]

Theoretically, the quantum yield Φ_{em} can be expressed as follows:

$$\Phi_{em} = \frac{k_r}{k_r + k_{nr}} \quad (1)$$

where

- k_r, radiative deactivation rate constant.
- k_{nr}, nonradiative deactivation rata constant.

Therefore, larger k_r and smaller k_{nr} would improve quantum yield Φ_{em}. On the one hand, owning to the π-accepting character of the P̂C ligand, the strongly coordinated phosphines are expected to be able to further destabilize the metal-centered ligand field d-d excited states that normally play a key role for guiding the quenching of emission,[64] therefore decreasing the nonradiative process.[65] As a result, the larger nonradiative constant (k_{nr}), that is, the highest quenching efficiency, of **1** can be rationalized by the weak bond between Iridium(III) metal and the P̂C ligand. And the quantum yield (Φ_{em}) can be speculated to be in the following order: $\Phi_{em}(\mathbf{2}) > \Phi_{em}(\mathbf{1})$. On the other hand, it is notable that from **3** to **2** and finally **1** the π-orbitals of the Np chromophore, with the progressively growing volume provided by the PH_2 and PPh_2 in **2** and **1**, respectively, reside relatively for away from the Ir metal center. Theoretically, the spin−orbit coupling is proportional to distance (r) to the six power (according to a qualitative approach for a hydrogen alike atom),[66] in which r is the distance between Ir and the ancillary chromophore. Therefore, **3** is expected to have stronger heavy atom−induced spin−orbit coupling, giving a much allowed $T_1 \rightarrow S_0$ transition and hence a larger radiative rate constant (k_r). Namely, it is reasonable to have the quantum yield in the following order, $\Phi_{em}(\mathbf{3}) > \Phi_{em}(\mathbf{2}) > \Phi_{em}(\mathbf{1})$. The result here is consistent with quantum yield expectation mentioned above.

According to Einstein theory of spontaneous emission, the radiative rate constant k_r can be expressed as:

$$k_r \propto E^3|M|^2 \quad (2)$$

where

- E, the emitting energy.
- M, the transition dipole moment, which relates to oscillator strength.

Previous work[67] has been proved that the transition dipole moment M plays a much more important role in emission process from the lowest triplet state. Because the transition metal is the pivotal factor that makes the spin−forbidden singlet−triplet transition possible, Li et al.[67] suggested that the radiative rate constant k_r could be correlated to the percentage of metal character (M%) in the emission process, in which the spin−orbit coupling matrix elements are expected to increase as the content of metal character increases in the corresponding excitation. It is possible to estimate the amount of metal character in the lowest singlet−triplet transition by looking at the product of the contribution of the corresponding TD-DFT eigenvector and the percentage of metal character (M%) involved in the transition, as claimed by De Angelis et al.[16] before. The calculated metal character for the corresponding excitation are summarized the last column in Table 6. With this assumption in mind, the k_r values could be rearranged in the following order: $k_r(\mathbf{3}) > k_r(\mathbf{2}) > k_r(\mathbf{1})$ according to the calculated metal content involved in the corresponding singlet−triplet transition. To sum up, it can be expected that **3** would be the one with the highest quantum efficiency among all the others in current investigation.

CONCLUSION

DFT calculations have been performed to investigate the geometries, electronic structures, the lowest-lying singlet absorptions and triplet emissions of **1** − **3**. Based on the detailed discussion above, the following conclusions can be drawn:

- Complexes **1**−**3** have similar electron density population. In singlet ground state, the HOMOs are localized mainly on Np ligands and Ir metal, while the LUMOs reside on fppy ligand.
- The lowest-lying absorption and emission are ligand-based charge−transfer transition with some mixture of MLCT transition. For **1**−**3**, absorptions and emissions involve charge−transfer transition between Np and fppy ligand via Ir metal center.
- The theoretically designed model **2** would emit at 563 nm with similar efficiency as that of **1**. Our calculation proved that the newly designed molecular **2** not only has the similar electronic structure but also the similar metal contribution involved in the emission transition, as compares to **1**. Thus we could conclude that the newly designed molecular **2** would be highly emission, too. For **1** and **2**, these two are different in the exact ancillary P̂C ligand, but they got the similar electronic structure properties and almost identical emission color. This means that the $\pi-\pi$ interaction between P̂C ligand and fppy ligand is not the main factor which keeps the high quantum efficiency of **1**. In fact, it is the P̂C ligand itself.
- Closer space arrangement of ancillary chromophore and Ir atom could further facilitate the overlap between π-orbital of ancillary ligand and d orbital of Ir atom, giving out a much allowed emission. Heavy metal participation is another factor to obtain higher quantum efficiency. From these points of view, complex **3** is expected to be highly emissive in deep blue at 470 nm.

We hope these theoretical studies could provide some inspiration in the design of highly efficient blue phosphorescent materials.

AUTHOR INFORMATION

Corresponding Author

*E-mail: zhanghx@mail.jlu.edu.cn.

ACKNOWLEDGMENT

This work was supported by the Natural Science Foundation of China (Grant Nos. 20973076 and 21003057).

REFERENCES

(1) Tsuboyama, A.; Iwawaki, H.; Furugori, M.; Mukaide, T.; Kamatani, J.; Igawa, S.; Moriyama, T.; Miura, S.; Takiguchi, T.; Okada, S.; Hoshino, M.; Ueno, K. *J. Am. Chem. Soc.* **2003**, *125*, 12971–12979.

(2) Lai, S.-W.; Che, C.-M. Luminescent Cyclometalated Diimine Platinum(II) Complexes: Photophysical Studies and Applications. In *Transition Metal and Rare Earth Compounds*; Yersin, H., Ed.; Springer Berlin: Heidelberg, 2004; Vol. 241, pp 27−63.

(3) Yersin, H. Triplet Emitters for OLED Applications. Mechanisms of Exciton Trapping and Control of Emission Properties. In *Transition Metal and Rare Earth Compounds*; Yersin, H., Ed.; Springer Berlin: Heidelberg, 2004; Vol. 241, pp 1−26.

(4) Mazzeo, M.; Vitale, V.; Della Sala, F.; Anni, M.; Barbarella, G.; Favaretto, L.; Sotgiu, G.; Cingolani, R.; Gigli, G. *Adv. Mater.* **2005**, *17*, 34–39.

(5) Chou, P.-T.; Chi, Y. *Chem.—Eur. J.* **2007**, *13*, 380–395.

(6) Jia, W.-L.; Bai, D.-R.; McCormick, T.; Liu, Q.-D.; Motala, M.; Wang, R.-Y.; Seward, C.; Tao, Y.; Wang, S. *Chem.—Eur. J.* **2004**, *10*, 994–1006.

(7) Rausch, A. F.; Thompson, M. E.; Yersin, H. *Inorg. Chem.* **2009**, *48*, 1928–1937.

(8) Adachi, C.; Baldo, M. A.; Thompson, M. E.; Forrest, S. R. *J. Appl. Phys.* **2001**, *90*, 5048–5051.

(9) Nazeeruddin, M. K.; Humphry-Baker, R.; Berner, D.; Rivier, S.; Zuppiroli, L.; Grätzel, M. *J. Am. Chem. Soc.* **2003**, *125*, 8790–8797.

(10) M., M.; A., C.; L., P.; T., G. M. *Handbook of Photochemistry*; CRC Press: Boca Raton, FL, 2006.

(11) Baldo, M. A.; Thompson, M. E.; Forrest, S. R. *Nature* **2000**, *403*, 750–753.

(12) Gu, X.; Fei, T.; Zhang, H.; Xu, H.; Yang, B.; Ma, Y.; Liu, X. *Eur. J. Inorg. Chem.* **2009**, *2009*, 2407–2414.

(13) Duan, J.; Sun, P.; Cheng, C. *Adv. Mater.* **2003**, *15*, 224–228.

(14) Slinker, J. D.; Koh, C. Y.; Malliaras, G. G.; Lowry, M. S.; Bernhard, S. *Appl. Phys. Lett.* **2005**, *86*, 173506.

(15) Zhou, G.; Wong, W.-Y.; Yao, B.; Xie, Z.; Wang, L. *Angew. Chem., Int. Ed.* **2007**, *46*, 1149–1151.

(16) De Angelis, F.; Fantacci, S.; Evans, N.; Klein, C.; Zakeeruddin, S. M.; Moser, J.-E.; Kalyanasundaram, K.; Bolink, H. J.; Grätzel, M.; Nazeeruddin, M. K. *Inorg. Chem.* **2007**, *46*, 5989–6001.

(17) Zhou, G.; Ho, C.-L.; Wong, W.-Y.; Wang, Q.; Ma, D.; Wang, L.; Lin, Z.; Marder, T. B.; Beeby, A. *Adv. Funct. Mater.* **2008**, *18*, 499–511.

(18) You, Y.; Park, S. Y. *Dalton Trans.* **2009**, *8*, 1267–1282.

(19) Lamansky, S.; Djurovich, P.; Murphy, D.; Abdel-Razzaq, F.; Kwong, R.; Tsyba, I.; Bortz, M.; Mui, B.; Bau, R.; Thompson, M. E. *Inorg. Chem.* **2001**, *40*, 1704–1711.

(20) Liu, T.; Xia, B.-H.; Zheng, Q.-C.; Zhou, X.; Pan, Q.-J.; Zhang, H.-X. *J. Comput. Chem.* **2010**, *31*, 628–638.

(21) Byun, Y.; Jeon, W. S.; Lee, T.-W.; Lyu, Y.-Y.; Chang, S.; Kwon, O.; Han, E.; Kim, H.; Kim, M.; Lee, H.-J.; Das, R. R. *Dalton Trans.* **2008**, 4732–4741.

(22) Lo, S.-C.; Harding, R. E.; Shipley, C. P.; Stevenson, S. G.; Burn, P. L.; Samuel, I. D. W. *J. Am. Chem. Soc.* **2009**, *131*, 16681–16688.

(23) Chen, L.; You, H.; Yang, C.; Zhang, X.; Qin, J.; Ma, D. *J. Mater. Chem.* **2006**, *16*, 3332–3339.

(24) Peng, T.; Bi, H.; Liu, Y.; Fan, Y.; Gao, H.; Wang, Y.; Hou, Z. *J. Mater. Chem.* **2009**, *19*, 8072–8074.

(25) Dedeian, K.; Shi, J.; Shepherd, N.; Forsythe, E.; Morton, D. C. *Inorg. Chem.* **2005**, *44*, 4445–4447.

(26) Du, B.-S.; Lin, C.-H.; Chi, Y.; Hung, J.-Y.; Chung, M.-W.; Lin, T.-Y.; Lee, G.-H.; Wong, K.-T.; Chou, P.-T.; Hung, W.-Y.; Chiu, H.-C. *Inorg. Chem.* **2010**, *49*, 8713–8723.

(27) Chen, Z.-Q.; Bian, Z.-Q.; Huang, C.-H. *Adv. Mater.* **2010**, *22*, 1534–1539.

(28) Shen, J. Y.; Lee, C. Y.; Huang, T.-H.; Lin, J. T.; Tao, Y.-T.; Chien, C.-H.; Tsai, C. *J. Mater. Chem.* **2005**, *15*, 2455–2463.

(29) Kim, S. O.; Lee, K. H.; Kim, G. Y.; Seo, J. H.; Kim, Y. K.; Yoon, S. S. *Synth. Met.* **2010**, *160*, 1259–1265.

(30) Mikami, A.; Koshiyama, T.; Tsubokawa, T. *Jpn. J. Appl. Phys.* **2005**, *44*, 608–612.

(31) Jabbour, G. E.; Kawabe, Y.; Shaheen, S. E.; Wang, J. F.; Morrell, M. M.; Kippelen, B.; Peyghambarian, N. *Appl. Phys. Lett.* **1997**, *71*, 1762–1764.

(32) Mikami, A.; Nishita, Y.; Iida, Y. *SID Symp. Dig. Tech. Pap.* **2006**, *37*, 1376–1379.

(33) Shen, L.; Zhang, H.-Y.; Ji, H.-F. *Org. Lett.* **2005**, *7*, 243–246.

(34) Burke, K.; Werschnik, J.; Gross, E. K. U. *J. Chem. Phys.* **2005**, *123*, 062206.

(35) Sousa, S. F.; Fernandes, P. A.; Ramos, M. J. a. *J. Phys. Chem. A* **2007**, *111*, 10439–10452.

(36) Zhang, X.-H.; Li, C.; Wang, W.-B.; Cheng, X.-X.; Wang, X.-S.; Zhang, B.-W. *J. Mater. Chem.* **2007**, *17*, 642–649.

(37) Ding, Y.; xiu Guo, J.; si Wang, X.; sha Liu, S.; cai Ma, F. *Chin. J. Chem. Phys.* **2009**, *22*, 269–274.

(38) Chen, Y.-G.; Yan, L.-K.; Hao, X.-R.; Liu, K.; Wang, X.-H.; Lu, P.-P. *Inorg. Chim. Acta* **2006**, *359*, 2550–2554.
(39) Li, X.-N.; Wu, Z.-J.; Li, X.-Y.; Zhang, H.-J.; Liu, X.-J. *J. Comput. Chem.* **2011**, *32*, 1033–1042.
(40) Parr, R. G. *Annu. Rev. Phys. Chem.* **1983**, *34*, 631–656.
(41) Kohn, W.; Sham, L. J. *Phys. Rev.* **1965**, *140*, A1133–A1138.
(42) Frisch, M. J. et al. *Gaussian 09*, Revision A.02; Gaussian Inc.: Wallingford, CT, 2009.
(43) Petersilka, M.; Gossmann, U. J.; Gross, E. K. U. *Phys. Rev. Lett.* **1996**, *76*, 1212–1215.
(44) Cossi, M.; Scalmani, G.; Rega, N.; Barone, V. *J. Chem. Phys.* **2002**, *117*, 43–54.
(45) Barone, V.; Cossi, M.; Tomasi, J. *J. Chem. Phys.* **1997**, *107*, 3210–3221.
(46) Hay, P. J.; Wadt, W. R. *J. Chem. Phys.* **1985**, *82*, 299–310.
(47) Shi, L.; Hong, B.; Guan, W.; Wu, Z.; Su, Z. *J. Phys. Chem. A* **2010**, *114*, 6559–6564.
(48) Nie, D.; Liu, Z.; Bian, Z.; Huang, C. *J. Mol. Struct.: THEOCHEM* **2008**, *861*, 97–102.
(49) Dolg, M.; Stoll, H.; Preuss, H.; Pitzer, R. M. *J. Phys. Chem.* **1993**, *97*, 5852–5859.
(50) Schuchardt, K. L.; Didier, B. T.; Elsethagen, T.; Sun, L.; Gurumoorthi, V.; Chase, J.; Li, J.; Windus, T. L. *J. Chem. Inf. Model* **2007**, *47*, 1045–1052.
(51) Feller, D. *J. Comput. Chem.* **1996**, *17*, 1571–1586.
(52) Dunning, T., Jr. *J. Chem. Phys.* **1989**, *90*, 1007.
(53) Foresman, J. B.; Head-Gordon, M.; Pople, J. A.; Frisch, M. J. *J. Phys. Chem.* **1992**, *96*, 135–149.
(54) Stanton, J. F.; Gauss, J.; Ishikawa, N.; Head-Gordon, M. *J. Chem. Phys.* **1995**, *103*, 4160–4174.
(55) Zhao, Y.; Truhlar, D. G. *J. Phys. Chem. A* **2006**, *110*, 5121–5129.
(56) Dreuw, A.; Head-Gordon, M. *Chem. Rev.* **2005**, *105*, 4009–4037.
(57) Li, X.-N.; Liu, X.-J.; Wu, Z.-J.; Zhang, H.-J. *J. Phys. Chem. A* **2008**, *112*, 11190–11197.
(58) Li, X.-N.; Wu, Z.-J.; Liu, X.-J.; Zhang, H.-J. *J. Phys. Chem. A* **2010**, *114*, 9300–9308.
(59) Li, X.-N.; Wu, Z.-J.; Si, Z.-J.; Zhang, H.-J.; Zhou, L.; Liu, X.-J. *Inorg. Chem.* **2009**, *48*, 7740–7749.
(60) Jacquemin, D.; Perpète, E. A.; Ciofini, I.; Adamo, C. *Acc. Chem. Res.* **2009**, *42*, 326–334.
(61) Tognetti, V.; Floch, P. L.; Adamo, C. *J. Comput. Chem.* **2009**, *31*, 1053–1062.
(62) Lee, C.; Yang, W.; Parr, R. G. *Phys. Rev. B* **1988**, *37*, 785–789.
(63) Lee, T.-C.; Chang, C.-F.; Chiu, Y.-C.; Chi, Y.; Chan, T.-Y.; Cheng, Y.-M.; Lai, C.-H.; Chou, P.-T.; Lee, G.-H.; Chien, C.-H.; Shu, C.-F.; Leonhardt, J. *Chem. Asian J.* **2009**, *4*, 742–753.
(64) Hung, J.-Y.; Lin, C.-H.; Chi, Y.; Chung, M.-W.; Chen, Y.-J.; Lee, G.-H.; Chou, P.-T.; Chen, C.-C.; Wu, C.-C. *J. Mater. Chem.* **2010**, *20*, 7682–7693.
(65) Chiu, Y.-C.; Lin, C.-H.; Hung, J.-Y.; Chi, Y.; Cheng, Y.-M.; Wang, K.-W.; Chung, M.-W.; Lee, G.-H.; Chou, P.-T. *Inorg. Chem.* **2009**, *48*, 8164–8172.
(66) McGlynn, S. P.; Azumi, T.; Kinoshita, M. *Molecular Spectroscopy of the Triplet State*; Prentice Hall: Englewood Cliffs, NJ, 1969; p 434.
(67) Li, X.; Zhang, Q.; Tu, Y.; Agren, H.; Tian, H. *Phys. Chem. Chem. Phys.* **2010**, *12*, 13730–13736.